A Reliable Successive Relaying Protocol

Ertuğrul Başar, *Member, IEEE,* Ümit Aygölü, *Member, IEEE,* Erdal Panayırcı, *Life Fellow, IEEE,* and H. Vincent Poor, *Fellow, IEEE*

***Abstract*—Successive relaying has recently emerged as an effective technique for cooperative networks and provides significant improvements in bandwidth efficiency over traditional relaying techniques; however, to achieve full-diversity, the available successive relaying protocols generally assume noise-free source-relay and interference-free inter-relay channels. In this paper, a novel successive relaying protocol is proposed for N-relay wireless networks by removing these optimistic assumptions. The proposed protocol benefits from distributed space-time block codes (STBCs) with coordinate interleaving and relay selection. It achieves a diversity order of two and high transmission rate under realistic network conditions with single-symbol maximum likelihood (ML) detection. A general N-relay signaling protocol is presented, and specific design examples are given for $N = 2$, 3 and 4-relay cooperative networks. The average symbol error probability (ASEP) is analytically derived and shown to match with computer simulation results. It is also shown via computer simulations that the proposed scheme achieves significantly better error performance and is more robust to channel estimation errors than its counterparts given in the literature under realistic network conditions.**

***Index Terms*—Cooperative communications, coordinate interleaved orthogonal design (CIOD), successive relaying.**

I. Introduction

COOPERATIVE communications, which is capable of creating a virtual multi-antenna system for the mobile terminals of a relaying network equipped with single antennas, has appeared as a promising strategy in the past decade [1], [2], [3]. Generally, distributed space-time block codes (STBCs) can be used effectively for relaying networks to benefit from the diversity gains provided by this virtual multi-antenna system [2], [4]. One of the most challenging problems in the design of distributed STBCs arises from the half-duplex constraint that limits the wireless nodes' ability to transmit and receive simultaneously [5]. Therefore, in such a system, two transmission phases (a broadcast phase and a cooperation phase) are required to transfer the data from the source node to the destination node. Consequently, transmission rates of distributed STBCs cannot reach those of STBCs operating on conventional multiple-input multiple-output (MIMO) systems.

Manuscript received June 6, 2013; revised October 21, 2013 and January 6, 2014. The editor coordinating the review of this paper and approving it for publication was A. Ghrayeb.

E. Başar and Ü. Aygölü are with Istanbul Technical University, Faculty of Electrical and Electronics Engineering, 34469, Maslak, Istanbul, Turkey (e-mail: {basarer, aygolu}@itu.edu.tr).

E. Panayırcı is with Kadir Has University, Department of Electrical and Electronics Engineering, 34083, Cibali, Istanbul, Turkey (e-mail: eepanay@khas.edu.tr).

H. V. Poor is with the Department of Electrical Engineering, Princeton University, Princeton, NJ, 08544, USA (e-mail: poor@princeton.edu).

Digital Object Identifier 10.1109/TCOMM.2014.030214.130420

Two-path successive relaying has been recently proposed as an effective cooperative transmission strategy since it provides significant bandwidth efficiency improvement over the classical relaying methods [6], [7]. In two-path successive relaying, the loss in the transmission rate of traditional relaying protocols is recovered by continuous data transmission from the source node while the relay nodes transmit and listen alternately. Consequently, only $L + 1$ time intervals are required for the transmission of L information symbols, i.e., essentially full rate is achieved for larger values of L. A major drawback of the earlier protocols for successive relaying is the loss of full-diversity, which is sacrificed for high bandwidth efficiency. In order to achieve full-diversity while preserving high transmission rates, distributed STBCs with the decode-and-forward (DF) protocol have been considered for two-path relaying networks. In [8], an effective distributed STBC, which provides high-rate and full-diversity, has been proposed for two-path relaying. In this scheme, L information symbols are transfered from the source node to the destination node in $L + 2$ transmission intervals via two relays which listen (to the source node) or transmit (to the destination node) alternately. However, this code does not yield single symbol maximum likelihood (ML) detection, which makes its implementation complicated and costly. Recently, a distributed STBC based on the coordinate interleaved orthogonal design (CIOD), has been proposed for two-path relaying [9]. CIODs are special STBCs which provide single-symbol ML detection, full-diversity and full-rate for 3 and 4 transmit antennas in addition to 2 transmit antennas in contrast to the classical STBCs [10]. In [9], the CIOD for two transmit antennas is transmitted in a distributed fashion with successive relaying, and, consequently, full-rate and full-diversity is achieved with single-symbol ML detection. More recently, the concept of [8] has been extended to the three-relay case, and a new successive relaying protocol has been proposed for relaying networks [11]. In this protocol, $L + 3$ transmission intervals are employed to relay the symbols to the destination, and a diversity order of three is achieved with a proper design of the corresponding distributed STBC at the expense of sacrificing single-symbol ML detection.

The aforementioned schemes proposed in [8], [9] and [11] provide effective solutions for successive-relaying networks; however, their operations are based on the following two assumptions:

A1- The relays can correctly decode the symbols received from the source node, i.e., the channels between the source node and the relay nodes are noise-free.

A2- The inter-relay channels are very strong so that

the interference between relays can be successfully eliminated, i.e., the channels between relays are interference-free.

However, these two assumptions are over-optimistic and cannot hold for practical wireless networks since the channels between the source and relays are subject to fading and noise, and the channels between relays cannot be interference-free due to fading. In [8], a selective relaying protocol has been implemented to relax A1 where the instantaneous signal-to-noise ratio (SNR) levels of the received signals at the relay nodes are measured and compared with a threshold SNR value. Then the relay nodes whose instantaneous SNR values are higher than this threshold value take part in the cooperation. Furthermore, it has been assumed that these cooperating relays always make correct decisions. It has been shown that the schemes of [8] and [11] can achieve full-diversity under selection relaying and A2. An adaptive relaying scheme has been also proposed in [8] to further relax A2; however, relatively strong inter-relay channels are still assumed in this scheme. Furthermore, the schemes of [8] and [11] also assume that the source-relay channels are much stronger than the channels between the relays and destination, i.e., the relay nodes are much closer to the source node than to the destination node. The inter-relay interference (IRI) problem has been also investigated in the literature for amplify-and-forward (AF) two-path successive relaying networks [6] and some solutions have been proposed in [12] and [13]. However, IRI is still one of the major problems of DF successive relaying schemes. Moreover, the theoretical error performance analysis of DF successive relaying schemes is generally ignored due to the complexity of the network and the signaling protocols, and only approximate diversity order calculations and diversity-multiplexing tradeoff analyses are given in [8] and [14].

In this paper, we propose a novel successive DF relaying protocol for cooperative networks with $N(N>1)$ relays by completely removing the assumptions mentioned above (A1 and A2). Unlike the previous work described in the literature, the proposed protocol can achieve a diversity order of two in a realistic network environment in which relays can erroneously detect the received signals and interfere with each other, and yet, it can transfer data from the source node to the destination node via N relays in a reliable manner. The proposed protocol benefits from distributed STBCs with coordinate interleaving (CIODs) and allows single-symbol ML detection at all relay nodes and the destination node. Furthermore, the proposed scheme can transfer $2N-2$ information symbols over $2N-1$ time intervals; therefore its transmission rate approaches unity for higher numbers of relays. In order to achieve full-diversity at the destination of the proposed scheme, the relay nodes also achieve diversity by exploiting relay selection and distributed STBCs. Since the relay nodes achieve diversity, their decision errors do not effect the diversity order at the destination node; therefore, A1 can be removed safely by the proposed signaling protocol. On the other hand, the proposed signaling protocol also allows the removal of A2, since the interfering signals between relays have been reliably decoded (due to the diversity) at the other listening relays at the previous time slots; therefore, these interfering signals can be subtracted from the presently received signals to obtain the desired signals. Specific design examples are given for networks with $N=2$, 3 and 4 relays. First, the average symbol error probability (ASEP) of the proposed scheme is analytically evaluated using M-ary quadrature amplitude modulation (M-QAM) taking into account the erroneous decisions at relays and their effect on the destination, i.e. the error propagation, then an approximation of the ASEP is derived for a general N-relay case. It is shown that our theoretical results match very well with that of computer simulations. It is also shown by computer simulations that the proposed scheme achieves significantly better error performance and it is more robust to the channel estimation errors than its counterparts given in the literature under realistic network conditions.

The organization of the paper is as follows. In Section II, we give the system model and introduce the general signaling protocol of the proposed scheme. In Sections III and IV, design examples for networks with 2, 3 and 4 relays are presented, and their theoretical ASEP performance is evaluated. Section V provides an approximation for the ASEP of the general scheme with N relays. The simulation results and the performance comparisons are given in Section VI. Finally, Section VII includes the main conclusions of the paper*.

II. System Model and The Proposed Protocol

In this section, we define our system model and present the general successive relaying protocol for the considered N-relay wireless network. In Fig. 1, a relay network consisting of a source node S, N relay nodes $(R_1, R_2, \ldots, R_N)$ and a destination node D, is considered. Each node employs a single antenna and operates in half-duplex mode. We assume that there is not a direct link from S to D. h_{SR_i} and $h_{R_iD}, i=1,\ldots,N$, represent the wireless channel fading coefficient between S and R_i, and R_i and D, respectively, while the fading channel coefficient between R_i and R_j is represented by $h_{R_iR_j}$. All channels are assumed reciprocal in which fading channel coefficients remain unchanged for opposite directions of the same link. Previously, wireless channels with different statistics between nodes are considered in the literature; however, in this work, all wireless channels are assumed to be identically distributed, namely the real and imaginary parts of h_{SR_i}, h_{R_iD} and $h_{R_iR_j}$ follow the $\mathcal{N}\left(0,\frac{1}{2}\right)$ distribution. Squared absolute values of the corresponding fading channel coefficients are denoted by

$$h_i = \left|h_{SR_i}\right|^2,\ h_{i,j} = \left|h_{R_iR_j}\right|^2,\ g_i = \left|h_{R_iD}\right|^2 \qquad (1)$$

for $i,j=1,\ldots,N$. We assume that the h_{R_iD}'s are known at D, while h_{SR_i} is known at relay R_i for $i=1,\ldots,N$. We also assume that the $h_{R_iR_j}$'s are known at R_j. The zero-mean complex Gaussian noise samples at time slot t are denoted

Notation: For a complex variable $s=s^R+js^I$, s^R and s^I denote the real and imaginary parts of s, respectively, where $j=\sqrt{-1}$, and $(\cdot)^*$ denotes complex conjugation. $x\sim\mathcal{N}\left(\mu_x,\sigma_x^2\right)$ denotes the Gaussian distribution of a real random variable (r.v.) x with mean μ_x and variance σ_x^2, while $x\sim\mathcal{CN}\left(0,\sigma_x^2\right)$ denotes the circularly symmetric complex Gaussian distribution of x with variance σ_x^2. $Q(\cdot)$ denotes the tail probability of the standard Gaussian distribution. The cumulative and probability density functions (c.d.f. and p.d.f.) of the r.v. x are denoted by $F_x(x)$ and $f_x(x)$, respectively, while its moment generating function (m.g.f.) is denoted by $M_x(s)=E\{e^{sx}\}$, where $E\{\cdot\}$ stands for expectation.

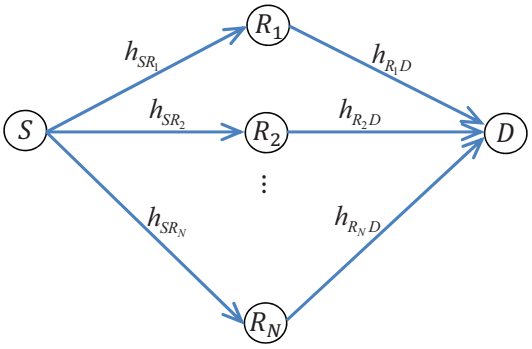

Fig. 1. The relay network model.

by $n_{R_i}(t)$ and $n_D(t)$ at R_i and D, respectively, and their variances are assumed to be N_0.

The proposed scheme is based on CIOD transmission with two transmit antennas (two relays, in our case) which can be represented by either of the following 2×2 transmission matrices [10]:

$$\begin{bmatrix} s_1^R + js_2^I & 0 \\ 0 & s_2^R + js_1^I \end{bmatrix} \tag{2}$$

$$\begin{bmatrix} s_2^R + js_1^I & 0 \\ 0 & s_1^R + js_2^I \end{bmatrix} \tag{3}$$

where the columns and the rows of (2) and (3) correspond to time slots and transmit antennas, respectively. $s_1 = s_1^R + js_1^I$ and $s_2 = s_2^R + js_2^I$ are two complex information symbols drawn from a rotated M-QAM constellation. Assume that a square M-QAM constellation with signal points $s = s^R + js^I$ where $s^R, s^I \in \left\{ \pm 1, \pm 3, \ldots, \pm\sqrt{M} - 1 \right\}$ is rotated by the amount of θ, the rotated signal constellation symbols are denoted by $s_\theta = se^{j\theta} = s_\theta^R + js_\theta^I$ whose real and imaginary components s_θ^R and s_θ^I take M distinct values from the set $\left\{ s^R \cos\theta - s^I \sin\theta \right\}$, where $\theta = 31.7°$ is the optimal rotation angle for square M-QAM which maximizes the coding gain [10]. Consequently, for a given s_θ^R $\left(s_\theta^I\right)$, s_θ^I $\left(s_\theta^R\right)$ can be determined uniquely. As an example, for 4-QAM, the rotated symbols with distinct real and imaginary parts are $s_\theta \in \{(-1.376 + j0.325), (-0.325 - j1.376), (0.325 + j1.376), (1.376 - j0.325)\}$, and if $s_\theta^R = -1.376$ is given for this constellation, we know that $s_\theta^I = 0.325$ and it is unique. Constellation rotation is required for CIODs to achieve full-diversity, while in our scheme it is also necessary to identify symbols from their real or imaginary parts.

For every $2N - 1$ time slots, a total of $2N - 2$ rotated information symbols $(s_1, s_2, \ldots, s_{2N-2})$ are transmitted from S. Considering that $h_1 > h_2 > \cdots > h_N$, those $2N - 2$ symbols are transferred from S to D according to the signaling protocol given in Table I, where $\uparrow, \downarrow$ and NA denote transmitting mode, receiving mode and idle mode in which there is neither transmission nor reception, respectively, and

$$c_i = \begin{cases} s_i^R + js_{i+1}^I & \text{odd } i \\ s_i^R + js_{i-1}^I & \text{even } i \end{cases} \tag{4}$$

represents the coordinate interleaved (CI) symbols for $i = 1, 2, \ldots, 2N - 2$. Note that the constellation rotation enables the symbols s_i and s_{i+1} (or s_{i-1}) to be identified from c_i for odd i (or even i).

As seen from Table I, for a given odd time slot $t = 1, 3, \ldots, 2N - 3$, S transmits $c_t = s_t^R + js_{t+1}^I$ to the relays, while at even time slots $t + 1 = 2, 4, \ldots, 2N - 2$, R_1, which has the strongest source-relay link, decodes s_t and s_{t+1} from c_t first, since each symbol can be identified by its real or imaginary part only thanks to the constellation rotation. Then, $c_{t+1} = s_{t+1}^R + js_t^I$ is formed and forwarded to the other relays and D by R_1. Since c_t and c_{t+1} have been received by the other relays at successive two time slots t and $t + 1$, the distributed CIOD signaling is implemented for these relays in the form of the CIOD transmission matrix given in (2). Distributed CIOD signaling is also implemented at D in the form of (3) since at odd time slot t $(t > 1)$, instead of receiving a new CI symbol from S, one of the relays $(R_{(t+1)/2})$ forwards $c_{t-2} = s_{t-2}^R + js_{t-1}^I$ to D which is the reformed version of the CI symbol $c_{t-1} = s_{t-1}^R + js_{t-2}^I$ transferred to D via R_1 in the previous even time slot $t - 1$. In other words, at consecutive two time slots $t - 1$ and t, D receives c_{t-1} and c_{t-2}, which are formed by the symbol pair (s_{t-2}, s_{t-1}), from R_1 and $R_{(t+1)/2}$, respectively, while at consecutive two time slots t and $t + 1$, before taking part in relaying, each relay receives c_t and c_{t+1} from S and R_1, respectively. This allows the implementation of distributed CIOD signaling (in the forms of the transmission matrices given in (2) and (3) for $R_2, \ldots, R_N$ and D, respectively) at all nodes of the network except R_1. On the other hand, R_1 benefits from relay selection since the channel between S and R_1 is the strongest in the considered scenario. As seen from Table I, at odd time slots t $(t > 1)$, the transmitting relay node causes interference to the other relays while listening to the new CI symbol from S. However, this interference can be reliably eliminated since the interfering CI symbol transmitted from this relay node has been already decoded reliably at the other relays which benefit from the diversity provided by CIOD detection. Therefore, unlike the previous techniques described in the literature, our scheme can achieve second order diversity while requiring neither perfect detection at relays nor interference-free inter-relay channels. The transmission rate of the proposed signaling protocol is found to be $R = (2N - 2)/(2N - 1)$ complex symbols per channel use (spcu), which approaches unity with increasing N; however, the complexity of the system (signaling overhead, synchronization, etc.) linearly increases in this case. Nevertheless, in real applications the number of relays employed in a communication systems is limited and the complexity of the systems due to the relays is not substantial.

In order to benefit from relay selection, in the general case, the relay having the strongest link to S, forwards the reformed version of CI symbol it received in the previous time slot, to other relays and D at even time slots. At the third time slot, the relay having the second strongest link to S supports the strongest relay, while at the fifth time slot, the relay having the third strongest link to S forwards its signal, and so on.

III. Proposed Successive Relaying for Two Relays

In this section, first, we apply the proposed successive relaying scheme for a wireless network having two relays $(N = 2)$, i.e., for the case of two-path relaying, and then we evaluate the ASEP of this scheme for a general M-QAM scheme.

TABLE I
PROPOSED SUCCESSIVE RELAYING PROTOCOL FOR N RELAYS.

Time	S	R_1	R_2	R_3	$\cdots$	R_{N-1}	R_N	D
1	$c_1\uparrow$	$c_1\downarrow$	$c_1\downarrow$	$c_1\downarrow$	$\cdots$	$c_1\downarrow$	$c_1\downarrow$	NA
2	NA	$c_2\uparrow$	$c_2\downarrow$	$c_2\downarrow$	$\cdots$	$c_2\downarrow$	$c_2\downarrow$	$c_2\downarrow$
3	$c_3\uparrow$	$c_3, c_1\downarrow$	$c_1\uparrow$	$c_3, c_1\downarrow$	$\cdots$	$c_3, c_1\downarrow$	$c_3, c_1\downarrow$	$c_1\downarrow$
4	NA	$c_4\uparrow$	NA	$c_4\downarrow$	$\cdots$	$c_4\downarrow$	$c_4\downarrow$	$c_4\downarrow$
5	$c_5\uparrow$	$c_5, c_3\downarrow$	NA	$c_3\uparrow$	$\cdots$	$c_5, c_3\downarrow$	$c_5, c_3\downarrow$	$c_3\downarrow$
$\vdots$	$\vdots$	$\vdots$	$\vdots$	$\vdots$	$\vdots$	$\vdots$	$\vdots$	$\vdots$
$2N-5$	$c_{2N-5}\uparrow$	$c_{2N-5}, c_{2N-7}\downarrow$	NA	NA	$\cdots$	$c_{2N-5}, c_{2N-7}\downarrow$	$c_{2N-5}, c_{2N-7}\downarrow$	$c_{2N-7}\downarrow$
$2N-4$	NA	$c_{2N-4}\uparrow$	NA	NA	$\cdots$	$c_{2N-4}\downarrow$	$c_{2N-4}\downarrow$	$c_{2N-4}\downarrow$
$2N-3$	$c_{2N-3}\uparrow$	$c_{2N-3}, c_{2N-5}\downarrow$	NA	NA	$\cdots$	$c_{2N-5}\uparrow$	$c_{2N-3}, c_{2N-5}\downarrow$	$c_{2N-5}\downarrow$
$2N-2$	NA	$c_{2N-2}\uparrow$	NA	NA	$\cdots$	NA	$c_{2N-2}\downarrow$	$c_{2N-2}\downarrow$
$2N-1$	NA	NA	NA	NA	$\cdots$	NA	$c_{2N-3}\uparrow$	$c_{2N-3}\downarrow$

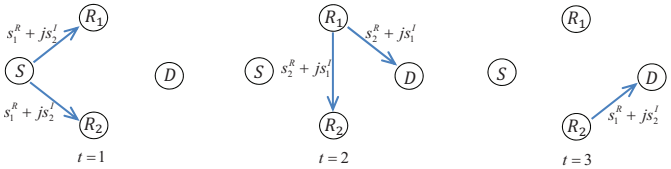

Fig. 2. Three phase successive relaying with stronger $S-R_1$ channel—two relays.

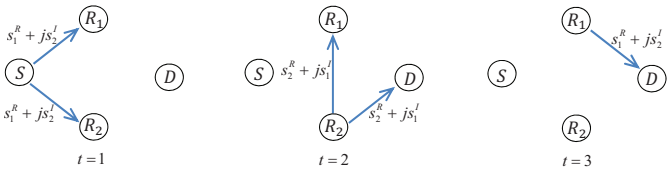

Fig. 3. Three phase successive relaying with stronger $S-R_2$ channel—two relays.

A. Protocol

In the proposed protocol given in Figs. 2-3, within every consecutive three time slots, two information symbols (s_1, s_2) drawn from a rotated M-QAM constellation are transmitted from S as follows: At the first time slot, S processes s_1 and s_2, and transmits the coordinate interleaved symbol $s_1^R + js_2^I$ to R_1 and R_2. If the $S-R_1$ channel is stronger than the $S-R_2$ channel, R_1 decodes s_1^R and s_2^I first, from which s_1 and s_2 are obtained since each symbol can be identified from its real or imaginary part only, which takes distinct values after the constellation rotation. Then R_1 forms and transmits the coordinate interleaved symbol $s_2^R + js_1^I$ to R_2 and D at the second time slot. As seen from (2), distributed CIOD signaling is achieved for R_2 after two time slots. At the third time slot, after detecting s_1 and s_2, R_2 transmits $s_1^R + js_2^I$ to D to create a virtual multiple-input single-output (MISO) system using the CIOD matrix given in (3) for D. As seen from Fig. 3, similar procedures can be applied when the $S-R_2$ channel is stronger than the $S-R_1$ channel. Note that a virtual MISO system is created for both D and one of the relays, while the other relay benefits from relay selection. Therefore, the overall diversity order of the system becomes two since not only D, but also R_1 and R_2 achieve a diversity order of two. On the other hand, the transmission rate of the proposed scheme with two relays is $2/3$ spcu since only two information symbols are transmitted in three time slots.

B. Evaluation of ASEP

We now evaluate the ASEP of the proposed scheme for general M-QAM. Without loss of generality, we can analyze the error performance of the signaling protocol given in Fig. 2 where the $S-R_1$ channel is stronger than the $S-R_2$ channel since the ASEP is the same for both cases. At the destination, the ASEP of the scheme given in Fig. 2 can be expressed as

$$P_D = \frac{1}{M}\sum\nolimits_{s}\sum\nolimits_{\hat{s}} P_D\left(s \to \hat{s}\right) \tag{5}$$

for $s \neq \hat{s}$ where $P_D\left(s \to \hat{s}\right)$ stands for the pairwise error probability (PEP) at the destination associated with detection of symbol $\hat{s}$ given that symbol s is transmitted.

The destination PEP $P_D\left(s \to \hat{s}\right)$ can be expressed as the sum of four probabilities related to the error events at the relays as $P_D\left(s \to \hat{s}\right) = P_1 + P_2 + P_3 + P_4$ with

$$P_1 = P_{R_1}^c\left(s\right) P_{R_2}^c\left(s \mid R_1^c\right) P_D\left(s \to \hat{s} \mid R_1^c, R_2^c\right),$$

$$P_2 = \sum_{\bar{s}, \bar{s}\neq s} P_{R_1}^c\left(s\right) P_{R_2}^e\left(s \to \bar{s} \mid R_1^c\right) P_D\left(s \to \hat{s} \mid R_1^c, R_2^e\right),$$

$$P_3 = \sum_{\tilde{s}, \tilde{s}\neq s} P_{R_1}^e\left(s \to \tilde{s}\right) P_{R_2}^c\left(s \mid R_1^e\right) P_D\left(s \to \hat{s} \mid R_1^e, R_2^c\right),$$

$$P_4 = \sum_{\tilde{s}, \tilde{s}\neq s}\sum_{\bar{s}, \bar{s}\neq s} P_{R_1}^e\left(s \to \tilde{s}\right) P_{R_2}^e\left(s \to \bar{s} \mid R_1^e\right) P_D\left(s \to \hat{s} \mid R_1^e, R_2^e\right)$$

where $P_{R_1}^c\left(s\right)$ is the probability of correct detection of s at R_1, $P_{R_2}^c\left(s \mid R_1^c\right)$ is the correct detection probability of s at R_2 conditioned on correct detection at R_1, $P_D\left(s \to \hat{s} \mid R_1^c, R_2^c\right)$ is the PEP at the destination conditioned on the correct detection of s at *both* relays, $P_{R_2}^e\left(s \to \bar{s} \mid R_1^c\right)$ is the PEP at R_2 conditioned on the correct detection of s at R_1, $P_D\left(s \to \hat{s} \mid R_1^c, R_2^e\right)$ is the PEP at the destination conditioned on correct detection of s at R_1 *and* erroneous detection of s to $\bar{s}$ at R_2, $P_{R_1}^e\left(s \to \tilde{s}\right)$ is the PEP at R_1, $P_{R_2}^c\left(s \mid R_1^e\right)$ is the probability of correct detection of s at R_2 conditioned on the erroneous detection of s to $\tilde{s}$ at R_1, $P_D\left(s \to \hat{s} \mid R_1^e, R_2^c\right)$ is the PEP at the destination conditioned on correct detection of s at R_2 *and* erroneous detection of s to $\tilde{s}$ at R_1, $P_{R_2}^e\left(s \to \bar{s} \mid R_1^e\right)$ is the PEP at R_2 conditioned on the erroneous detection of s to $\tilde{s}$ at R_1, and $P_D\left(s \to \hat{s} \mid R_1^e, R_2^e\right)$ is the PEP at the destination conditioned on the erroneous detection of s at *both* relays. Our analysis shows that the ASEP at D is dominated by the case where $\tilde{s} = \bar{s} = \hat{s}$, i.e., for the case where successive identical

erroneous detections occur in the relaying scheme. Therefore we obtain the following approximations:

$$P_2 \cong P^c_{R_1}(s) P^e_{R_2}(s \to \hat{s} \mid R^c_1) P_D(s \to \hat{s} \mid R^c_1, R^e_2),$$
$$P_3 \cong P^e_{R_1}(s \to \hat{s}) P^c_{R_2}(s \mid R^e_1) P_D(s \to \hat{s} \mid R^e_1, R^c_2),$$
$$P_4 \cong P^e_{R_1}(s \to \hat{s}) P^e_{R_2}(s \to \hat{s} \mid R^e_1) P_D(s \to \hat{s} \mid R^e_1, R^e_2).$$

We also observe that the ASEP at D is mainly dominated by P_1, P_2 and P_4, and the effect of P_3 can be ignored. This can be explained by the fact that $P^c_{R_2}(s \mid R^e_1) \ll P^e_{R_2}(s \to \hat{s} \mid R^e_1)$ while $P_D(s \to \hat{s} \mid R^e_1, R^c_2) \sim P_D(s \to \hat{s} \mid R^e_1, R^e_2)$. As it is shown in the sequel, independent of the SNR, the probability of symbol error increases dramatically at R_2 when R_1 makes a decision error. Therefore, the probability $P^c_{R_2}(s \mid R^e_1)$ can be neglected when compared to $P^e_{R_2}(s \to \hat{s} \mid R^e_1)$, and we can assume $P_3 \ll P_4$. Thus the ASEP can be basically rewritten as the sum of the three terms as

$$\begin{aligned} P_D(s \to \hat{s}) \cong\ & P^c_{R_1}(s) P^c_{R_2}(s \mid R^c_1) P_D(s \to \hat{s} \mid R^c_1, R^c_2) \\ & + P^c_{R_1}(s) P^e_{R_2}(s \to \hat{s} \mid R^c_1) P_D(s \to \hat{s} \mid R^c_1, R^e_2) \\ & + P^e_{R_1}(s \to \hat{s}) P^e_{R_2}(s \to \hat{s} \mid R^e_1) P_D(s \to \hat{s} \mid R^e_1, R^e_2). \quad (6) \end{aligned}$$

In order to obtain the ASEP, we have calculated (6) for $s = s_1$. The derivation of each term in (6) is quite lengthy. The details of the derivations are provided in Appendices A, B and C for the terms related to R_1 $\left(P^c_{R_1}(s), P^e_{R_1}(s \to \hat{s})\right)$, R_2 $\left(P^c_{R_2}(s \mid R^c_1), P^e_{R_2}(s \to \hat{s} \mid R^c_1), P^e_{R_2}(s \to \hat{s} \mid R^e_1)\right)$ and D $(P_D(s \to \hat{s} \mid R^c_1, R^c_2), P_D(s \to \hat{s} \mid R^c_1, R^e_2), P_D(s \to \hat{s} \mid R^e_1, R^e_2))$, respectively. In Appendix D, the diversity gain analysis for (6) is performed.

IV. The Proposed Protocol for Three and Four Relays

In this section, we investigate the implementation and the performance analysis of the proposed protocol for a wireless network with three and four relays.

A. Proposed Protocol for Three Relays

For a wireless network consisting of a source node (S), a destination node (D) and three relay nodes (R_1, R_2, R_3), during every five time slots, four information symbols (s_1, s_2, s_3, s_4) are transmitted from S. Assuming that $h_1 > h_2 > h_3$, these symbols are transferred from S to D according to the signaling protocol given in Table II. As seen from Table II, R_2 interferes with R_1 and R_3 at the third time slot, however, this interference can be eliminated in a reliable way since both R_1 and R_3 obtain s_1 and s_2 after the first two time slots with diversity (R_1 benefits from relay selection and R_2 can be considered as the receiver of a MISO system employing CIOD for two transmit antennas). For this case, the average destination SEP can be evaluated as

$$P_D = \frac{\text{ASEP}(s_1) + \text{ASEP}(s_3)}{2} \quad (7)$$

where $\text{ASEP}(s_i) = \frac{1}{M} \sum_{s_i} \sum_{\hat{s}_i} P_D(s_i \to \hat{s}_i)$, $i = 1, 3$, since symbol pairs (s_1, s_2) and (s_3, s_4) experience channels with different statistics. $P_D(s_1 \to \hat{s}_1)$ can be calculated by (6), while by neglecting the effect of the interference, $P_D(s_3 \to \hat{s}_3)$ can be calculated similarly from

$$\begin{aligned} P_D(s_3 \to \hat{s}_3) \cong\ & P^c_{R_1}(s_3) P^c_{R_3}(s_3 \mid R^c_1) P_D(s_3 \to \hat{s}_3 \mid R^c_1, R^c_3) \\ & + P^c_{R_1}(s_3) P^e_{R_3}(s_3 \to \hat{s}_3 \mid R^c_1) P_D(s_3 \to \hat{s}_3 \mid R^c_1, R^e_3) \\ & + P^e_{R_1}(s_3 \to \hat{s}_3) P^e_{R_3}(s_3 \to \hat{s}_3 \mid R^e_1) P_D(s_3 \to \hat{s}_3 \mid R^e_1, R^e_3). \end{aligned} \quad (8)$$

In order to obtain the ASEP for the three-relay case, considering the order statistics, the derivations for the terms in (7) are given in Appendix E.

TABLE II
Proposed Successive Relaying Protocol for Three Relays

Time	S	R_1	R_2	R_3	D
1	$c_1 \uparrow$	$c_1 \downarrow$	$c_1 \downarrow$	$c_1 \downarrow$	NA
2	NA	$c_2 \uparrow$	$c_2 \downarrow$	$c_2 \downarrow$	$c_2 \downarrow$
3	$c_3 \uparrow$	$c_3, c_1 \downarrow$	$c_1 \uparrow$	$c_3, c_1 \downarrow$	$c_1 \downarrow$
4	NA	$c_4 \uparrow$	NA	$c_4 \downarrow$	$c_4 \downarrow$
5	NA	NA	NA	$c_3 \uparrow$	$c_3 \downarrow$

TABLE III
Proposed Successive Relaying Protocol for Four Relays

Time	S	R_1	R_2	R_3	R_4	D
1	$c_1 \uparrow$	$c_1 \downarrow$	$c_1 \downarrow$	$c_1 \downarrow$	$c_1 \downarrow$	NA
2	NA	$c_2 \uparrow$	$c_2 \downarrow$	$c_2 \downarrow$	$c_2 \downarrow$	$c_2 \downarrow$
3	$c_3 \uparrow$	$c_3, c_1 \downarrow$	$c_1 \uparrow$	$c_3, c_1 \downarrow$	$c_3, c_1 \downarrow$	$c_1 \downarrow$
4	NA	$c_4 \uparrow$	NA	$c_4 \downarrow$	$c_4 \downarrow$	$c_4 \downarrow$
5	$c_5 \uparrow$	$c_5, c_3 \downarrow$	NA	$c_3 \uparrow$	$c_5, c_3 \downarrow$	$c_3 \downarrow$
6	NA	$c_6 \uparrow$	NA	NA	$c_6 \downarrow$	$c_6 \downarrow$
7	NA	NA	NA	NA	$c_5 \uparrow$	$c_5 \downarrow$

B. Proposed Protocol for Four Relays

For a wireless network consisting of a source node (S), a destination node (D) and four relay nodes (R_1, R_2, R_3, R_4), during every five time slots, six information symbols $(s_1, s_2, \ldots, s_6)$ are transmitted from S according to the proposed protocol. Assuming that $h_1 > h_2 > h_3 > h_4$, these symbols are transferred from S to D according to the signaling protocol given in Table III. For this case, the average destination SEP can be evaluated as

$$P_D = \frac{\text{ASEP}(s_1) + \text{ASEP}(s_3) + \text{ASEP}(s_5)}{3} \quad (9)$$

where $\text{ASEP}(s_i), i = 1, 3, 5$ are defined in (7). Here, by neglecting the effect of interference between relays, $P_D(s_1 \to \hat{s}_1)$ and $P_D(s_3 \to \hat{s}_3)$ can be calculated from (6) and (8), respectively, while $P_D(s_5 \to \hat{s}_5)$ can be calculated from

$$\begin{aligned} P_D(s_5 \to \hat{s}_5) \cong\ & P^c_{R_1}(s_5) P^c_{R_4}(s_5 \mid R^c_1) P_D(s_5 \to \hat{s}_5 \mid R^c_1, R^c_4) \\ & + P^c_{R_1}(s_5) P^e_{R_4}(s_5 \to \hat{s}_5 \mid R^c_1) P_D(s_5 \to \hat{s}_5 \mid R^c_1, R^e_4) \\ & + P^e_{R_1}(s_5 \to \hat{s}_5) P^e_{R_4}(s_5 \to \hat{s}_5 \mid R^e_1) P_D(s_5 \to \hat{s}_5 \mid R^e_1, R^e_4). \end{aligned} \quad (10)$$

Considering the new order statistics, corresponding new probability values can be obtained in closed form similar to the three-relay case derivations given in Appendix E.

V. Approximate ASEP of the Proposed Scheme with N Relays

In this section, by generalizing the concepts developed for $N = 2, 3$ and 4 so far, we provide an approximate ASEP expression for the N-relay scheme.

For N relays, by neglecting the effects of the interference between relay nodes, the average destination SEP can be evaluated as

$$P_D = \frac{\sum_{i=1}^{N-1} \text{ASEP}\left(s_{2i-1}\right)}{N-1} \tag{11}$$

where $\text{ASEP}\left(s_i\right)$ is as defined in (7). Considering the case where $h_1 > h_2 > \cdots > h_N$, we obtain $\text{ASEP}\left(s_1\right) < \text{ASEP}\left(s_3\right) < \cdots < \text{ASEP}\left(s_{2N-3}\right)$, since s_i is transfered to D via R_1 and $R_{(i+3)/2}$ for $i = 1, 3, \ldots, 2N-3$. In other words, the probability of error will be lower for the symbols transfered to D via relays with stronger source-relay channels. Therefore, for simplicity, we can approximate (11) by

$$P_D \approx \frac{\text{ASEP}\left(s_1\right) + \text{ASEP}\left(s_{(2N-3)}\right)}{2} \tag{12}$$

which considers the ASEP of the strongest symbol $\left(s_1\right)$ and the weakest symbol $\left(s_{(2N-3)}\right)$ only, and takes the average of these two probabilities. The calculations for the terms of (12) are provided in Appendix F.

VI. Numerical Results

In this section, we present our theoretical as well as Monte Carlo simulation results for the proposed successive relaying systems with two, three and four relays and make comparisons with the reference systems given in the literature, under the quasi-static uncorrelated Rayleigh fading channel assumption. The bit error rate (BER) and the symbol error rate (SER) performance of these systems was evaluated by Monte Carlo simulations as a function of the average SNR per bit (E_b/N_0). Unless specified otherwise, we consider unconstrained channels where the wireless channels between S and the relay nodes, the relay nodes and D, and inter-relays are independent and identically distributed with circularly symmetrical and zero-mean unit variance complex Gaussian distributions. For comparison purposes, we also consider strong inter-relay channels with variances $\sigma_R^2 > 1$.

A. Theoretical Results

In Fig. 4, the theoretical ASEP curves and the computer simulation results are shown for the proposed successive relaying scheme with two relays using 4-, 16- and 64-QAM modulations. As seen from Fig. 4, the theoretical and the computer simulation results become very close to each other with increasing SNR, and therefore support our in-depth analyses of Section III.B.

In Fig. 5(a), we provide the theoretical ASEP curve of the proposed signaling protocol for three relays which is obtained from (7) by averaging the ASEP of the symbols s_1 and s_3 and compare this curve with the one obtained through Monte Carlo simulations. As seen from this figure, unlike the two-relay case, there is an approximately 0.6 dB gap in terms of the SNR required for a target SER value between the theoretical and computer simulation curves in favor of the former since our theoretical analyses do not consider the effect of the interference between relays for this case. Nevertheless, we conclude from Fig. 5(a) that the proposed scheme is quite robust to the negative effects of the interference between the relays since its error performance is worsened only by 0.6 dB compared to the interference-free case.

We extend our analysis to the four-relay case in Fig. 5(b). The theoretical ASEP of the proposed scheme with four relays is obtained from (9) which takes the average of the ASEP of the symbols s_1, s_3 and s_5. In order to check its accuracy, we also show the approximate ASEP curve of the proposed scheme for N relays obtained from (12) by taking $N = 4$ which approximates the SER by averaging the ASEP of s_1 (the strongest symbol) and s_5 (the weakest symbol) only. We observe from Fig. 5(b) that the difference in SNR between the theoretical curve and computer simulation result

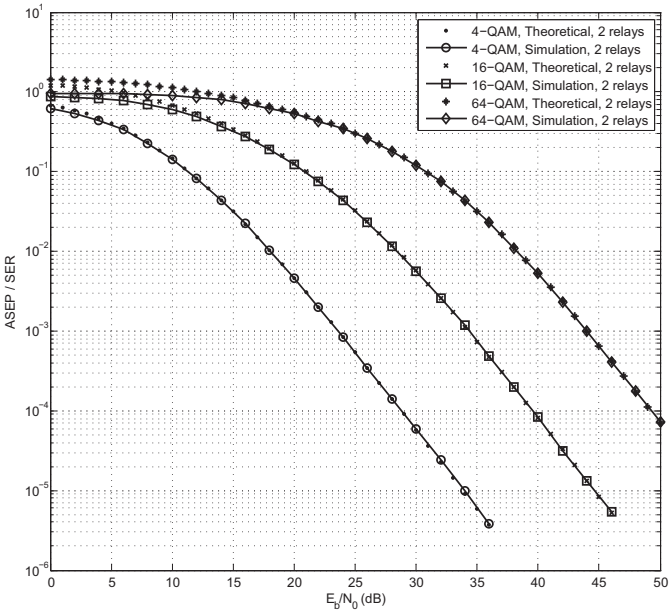

Fig. 4. Theoretical performance curves for the new scheme with two relays.

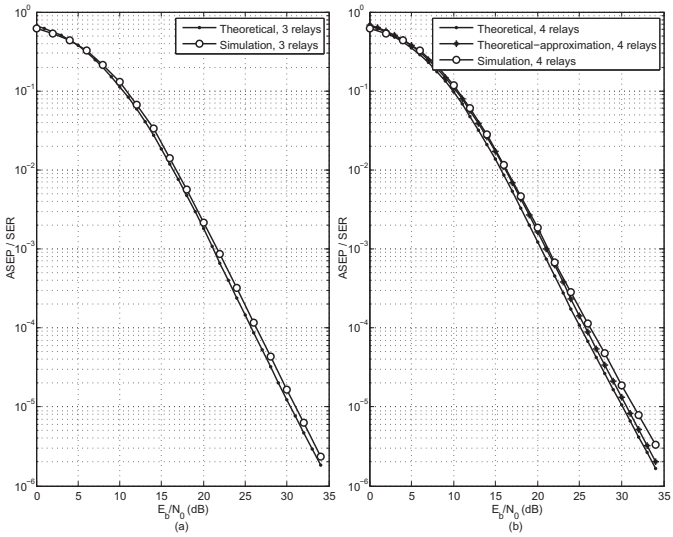

Fig. 5. Theoretical performance curves for the new scheme with (a) three and (b) four relays.

is larger (appr. 1.2 dB) than that of the three-relay case since the proposed protocol for four relays suffers from more interference due to the increased signaling traffic between S and D; however, it may be still considered robust against interference. On the other hand, we also observe from Fig. 5(b) that the approximation of the ASEP obtained from (12) is quite reasonable and can be used as an effective tool to predict the error performance of the proposed scheme in the general N-relay case.

B. Comparisons with Reference Schemes

In Fig. 6, we consider a two-relay network and provide the BER performance curves of the proposed scheme, the scheme of [8] and the scheme of [9] with and without error-free relays. It should be noted that the scheme of [9] with error-free relays is equivalent to the classical CIOD transmission and provides a performance benchmark for systems operating on realistic channel conditions. We employ 4-QAM modulation and ML detection for all systems. Note that, we apply selection relaying for the scheme of [8], where the threshold SNR is chosen as 12 dB. To achieve the same transmission rate of $2/3$ spcu for the schemes of [8] and [9], four $(L = 4)$ and two $(L = 2)$ information symbols have been transmitted from S in succession, respectively. We consider realistic network conditions in which relays can make erroneous detections for all schemes except the classical CIOD transmission. We also assume that two relays interfere with each other, where the variance of the inter-relay channels $\left(\sigma_R^2\right)$ is either 1 (strong inter-relay interference) or 8 (weak inter-relay interference). As seen from Fig. 6, without perfect decoding at the relays, the schemes of [8] and [9] cannot achieve full diversity while the proposed scheme does and it provides a significant improvement in BER performance. We also observe from Fig. 6 that the reference CIOD (scheme of [9] with error-free relays) and the proposed scheme achieve the same diversity order of two; however, the difference in the error performance can be explained by the additional errors at the relay nodes which increase the overall ASEP at the destination of the proposed scheme. It is important to note that the BER performance of the scheme of [8] is improved when the condition of the inter-relay channel gets better $\left(\sigma_R^2 = 8\right)$, however, the devastating effects of the inter-relay interference and the erroneous detections of the relays prevent it from achieving full-diversity at D.

We consider two and three-relay networks in Fig. 7 and provide the BER performance curves of the proposed scheme for $N = 3$, the scheme of [8], the scheme of [9] and the scheme of [11]. For the reference systems, the corresponding L values are adjusted accordingly so that all schemes except the scheme of [11], whose transmission rate is $8/11(0.73)$ spcu, achieve $4/5$ spcu. Similarly, we consider 4-QAM modulation, ML detection and realistic network conditions for all schemes, and apply selection relaying for the schemes of [8] and [11]. As seen from this figure, even with strong inter-relay channels, the schemes of [9] and [11] cannot achieve full-diversity under realistic network conditions, and they are outperformed by the proposed scheme. We observe from Fig. 7 that the proposed scheme with $N = 3$ exhibits

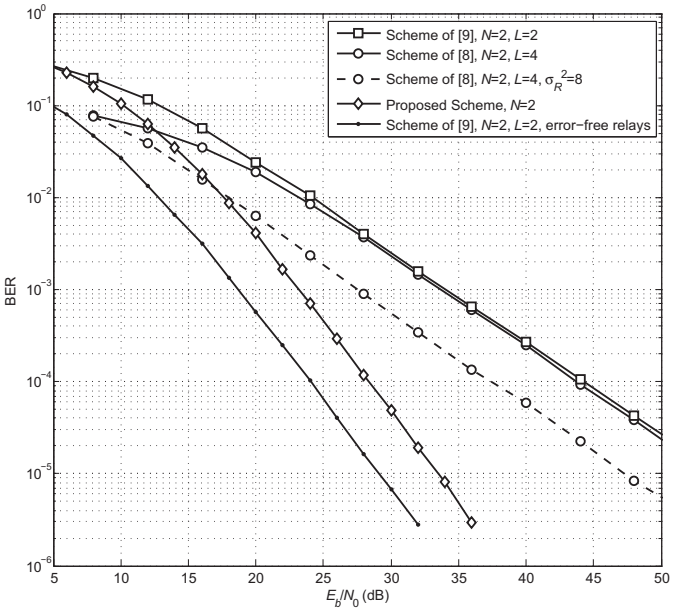

Fig. 6. Performance of the proposed protocol, the scheme of [8] and the scheme of [9] for a two-relay network and $2/3$ spcu.

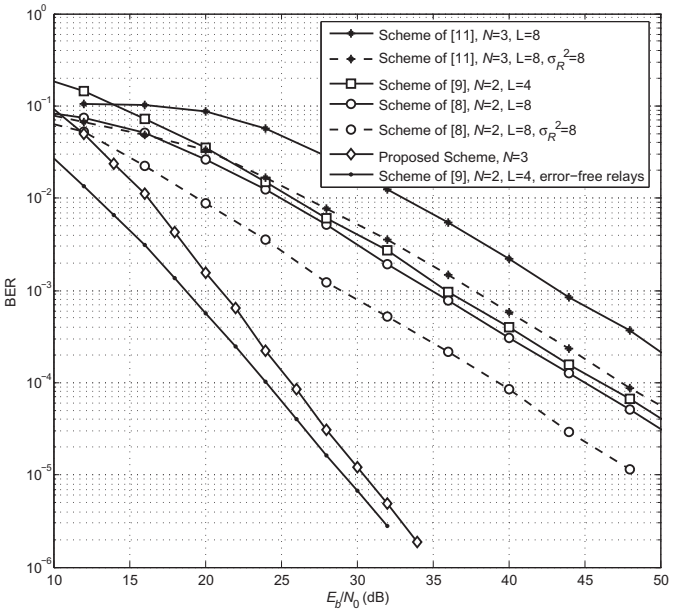

Fig. 7. Performance of the proposed protocol, and the schemes of [8], [9] and [11] for two and three-relay networks and $4/5$ spcu.

closer BER performance compared to the classical CIOD transmission (i.e., the scheme of [9] with error-free relays) and can achieve much better BER performance with a lower ML decoding complexity than the reference schemes when the wireless channels between the relay nodes undergo fading and consequently are subject to erroneous decisions.

C. Proposed Protocol Under Channel Estimation Errors

In this subsection, we investigate the performance of the proposed protocol in the presence of imperfect channel state information (CSI). When the corresponding wireless channel coefficients are estimated by the widely-used least squares (LS) channel estimators at the relay nodes and the destination, the estimation error model has the form $\hat{h}_{SR_i} = h_{SR_i} + \epsilon_{SR_i}$,

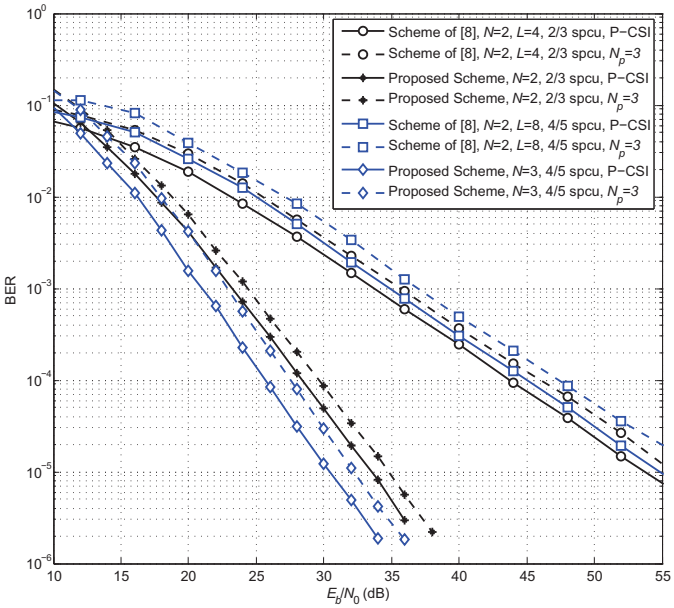

Fig. 8. Performance of the proposed protocol and scheme of [8] with imperfect CSI.

$\hat{h}_{R_iD} = h_{R_iD} + \epsilon_{R_iD}$, $\hat{h}_{R_iR_j} = h_{R_iR_j} + \epsilon_{R_iR_j}$ for $i, j = 1, \ldots, N$, where ϵ_{SR_i}, ϵ_{R_iD} and $\epsilon_{R_iR_j}$ represent the channel estimation errors which are independent from the corresponding wireless coefficients and from each other, and distributed according to $\mathcal{CN}\left(0, \sigma_\epsilon^2\right)$ [15]. We assume that the variance of the estimation error is adjusted according to the SNR as $\sigma_\epsilon^2 = 1/\left(N_p E_b/N_0\right)$ where N_p depends on the number of pilot symbols used in training and the chosen estimation method [16]. We consider the mismatched ML receivers in which the relay and the destination use the estimated channel fading coefficients in the perfect CSI (P-CSI) ML decision metrics† instead of the exact channel coefficients since these coefficients are imperfectly estimated and unknown to them. In Fig. 8, we compare the performance of the proposed protocol with the best reference system (scheme of [8]) under channel estimation errors. As seen from Fig. 8, the proposed protocol is more robust to the channel estimation errors than the scheme of [8] since for a BER value of 10^{-4}, compared to the case of P-CSI, the degradation amounts in BER performance are equal to 1.3 dB and 1.8 dB for the proposed protocol with $2/3$ and $4/5$ spcu, respectively, while these values are equal to 2.2 dB and 2.6 dB for the scheme of [8] with $2/3$ and $4/5$ spcu, respectively. We also observe from Fig. 8 that the proposed scheme preserves its full diversity in the presence of channel estimation errors.

VII. Conclusion

A novel as well as reliable successive relaying protocol, which can achieve high-rate and a diversity order of two, has been proposed for N-relay networks operating under realistic channel conditions in which the relays make decision errors and interfere with each other. The proposed protocol can be applied to practical networks in which there is not a direct transmission from the source node to the destination node, and the in-between relay nodes support the transmission. The theoretical error performance of the proposed signaling scheme has been derived after comprehensive calculations which consider the effects of error propagation. It has been shown by computer simulations that i) our theoretical analyses provide very accurate results, and ii) the proposed scheme achieves significantly better error performance than its counterparts given in the literature under realistic network conditions. In our future work, we plan to focus on the modification/development of the proposed protocol to increase its transmission rate over unity primarily for 2- and 3-relay networks as well as determining the receiver performance with theoretical tools in the presence of the channel estimation errors.

Appendix A
Calculation of Probabilities Related to R_1 $(N = 2)$
$P^c_{R_1}(s), P^e_{R_1}(s \to \hat{s})$

Without loss of generality, we consider the case in which the $S - R_1$ channel is stronger than the $S - R_2$ channel, i.e., $h_1 > h_2$. Since the p.d.f. of the jth order statistic x_j is given as [17]

$$f_{x_j}(x) = \frac{n!}{(j-1)!\,(n-j)!} f_x(x) \left[F_x(x)\right]^{j-1} \left[1 - F_x(x)\right]^{n-j} \tag{13}$$

where $x_1, x_2, \ldots, x_n$ are from a population with p.d.f. $f_x(x)$ and c.d.f. $F_x(x)$, we obtain $f_{h_1}(h_1) = 2\left(1 - e^{-h_1}\right)e^{-h_1}, h_1 > 0$ and $f_{h_2}(h_2) = 2e^{-2h_2}, h_2 > 0$.

i) $P^c_{R_1}(s_1)$: The received signal at R_1 for $t = 1$ is given as

$$r_{R_1}(1) = h_{SR_1}\left(s_1^R + j s_2^I\right) + n_{R_1}(1). \tag{14}$$

Thanks to coordinate interleaving, this signal can be expressed as follows for independent detection of s_1^R and s_2^I:

$$\begin{bmatrix} r^R_{R_1}(1) \\ r^I_{R_1}(1) \end{bmatrix} = \begin{bmatrix} h^R_{SR_1} & -h^I_{SR_1} \\ h^I_{SR_1} & h^R_{SR_1} \end{bmatrix} \begin{bmatrix} s_1^R \\ s_2^I \end{bmatrix} + \begin{bmatrix} n^R_{R_1}(1) \\ n^I_{R_1}(1) \end{bmatrix}. \tag{15}$$

For independent detection of s_1^R, R_1 obtains

$$y_{R_1} = h^R_{SR_1} r^R_{R_1}(1) + h^I_{SR_1} r^I_{R_1}(1) = h_1 s_1^R + w_{R_1} \tag{16}$$

where $w_{R_1} \triangleq h^R_{SR_1} n^R_{R_1}(1) + h^I_{SR_1} n^I_{R_1}(1)$ and h_1 is defined in (1). Therefore, the detection problem of s_1^R becomes the detection of a modified M-PAM signal subject to fading‡. When an M-QAM constellation with signal points $s = s^R + j s^I$ where $s^R, s^I \in \left\{\pm 1, \pm 3, \ldots, \pm\sqrt{M} - 1\right\}$ is rotated for CIOD, s_1^R takes elements from $s_1^R \in \left\{s^R \cos\theta + s^I \sin\theta\right\}$, where $\theta = \frac{1}{2}\tan^{-1}(2)$ is the optimal rotation angle for square M-QAM that maximizes the coding gain [10]. As an example, for 4-QAM, we have $s_1^R \in \{-\cos\theta - \sin\theta, -\cos\theta + \sin\theta, \cos\theta - \sin\theta, \cos\theta + \sin\theta\}$. Let us denote the possible values of s_1^R in ascending order as $a_1, a_2, \ldots, a_M$. Considering the transmission model given in (16), we have M decision intervals separated by the threshold values (normalized by h_1) $\lambda_1, \lambda_2, \ldots, \lambda_{M-1}$. As an example for 4-QAM, we have $\lambda_1 = -\cos\theta, \lambda_2 = 0, \lambda_3 = \cos\theta$.

†CIOD detection based ML decision metrics for the proposed protocol can be found in Appendices A, B (for the relays) and C (for the destination).

‡For independent detection of s_2^I, R_1 obtains $z_{R_1} = -h^I_{SR_1} r^R_{R_1}(1) + h^R_{SR_1} r^I_{R_1}(1)$.

Considering that w_{R_1} in (16) is distributed as $\mathcal{N}(0,\psi^2)$, where $\psi^2=\sigma^2 h_1$ and $\sigma^2=N_0/2$, the correct detection probability for $a_i, i=1,\ldots,M$ conditioned on h_1 can be given as

$$P^c_{R_1}(a_i)\Big|_{h_1}=\begin{cases}\int_{-\infty}^{h_1\lambda_1} f_{y_{R_1}}(y_{R_1}\mid a_1,h_1)\,dy_{R_1}, & i=1, i=M\\ \int_{h_1\lambda_{i-1}}^{h_1\lambda_i} f_{y_{R_1}}(y_{R_1}\mid a_i,h_1)\,dy_{R_1}, & \text{o.w.}\end{cases} \tag{17}$$

where conditioned on a_i and h_1, y_{R_1} follows the $\mathcal{N}\left(h_1 a_i,\psi^2\right)$ distribution for all i. Simple manipulation gives

$$P^c_{R_1}(a_i)\Big|_{h_1}=\begin{cases}1-Q\left(\frac{h_1(\lambda_1-a_1)}{\psi}\right), & i=1,\ i=M\\ 1-Q\left(\frac{h_1(a_i-\lambda_{i-1})}{\psi}\right)-Q\left(\frac{h_1(\lambda_i-a_i)}{\psi}\right), & \text{o.w.}\end{cases} \tag{18}$$

In order to obtain the unconditional correct detection probability for a_i, we have to integrate $P^c_{R_1}(a_i)\big|_{h_1}$ over the p.d.f. of h_1. Using the alternative form of the Q-function

$$Q(x)=\frac{1}{\pi}\int_0^{\pi/2}\exp\left(-\frac{x^2}{2\sin^2\theta}\right)d\theta \tag{19}$$

and considering the m.g.f. of h_1 given as $M_{h_1}(s)=2/(2-3s+s^2)$ the unconditional correct detection probability for a_i is obtained as follows:

$$P^c_{R_1}(a_i)=\begin{cases}1-q\left(\frac{(\lambda_1-a_1)^2}{N_0}\right), & i=1, i=M\\ 1-q\left(\frac{(a_i-\lambda_{i-1})^2}{N_0}\right)-q\left(\frac{(\lambda_i-a_i)^2}{N_0}\right), & \text{o.w.}\end{cases} \tag{20}$$

where

$$q(x)\triangleq\frac{1}{\pi}\int_0^{\pi/2}M_{h_1}\left(\frac{-x}{\sin^2\theta}\right)d\theta=\frac{1}{2}\left(1-\frac{2}{\sqrt{1+\frac{1}{x}}}+\frac{1}{\sqrt{1+\frac{2}{x}}}\right). \tag{21}$$

ii) $P^e_{R_1}(s_1\to\hat{s}_1)$: For the signaling scheme of (16), the pairwise SEP of detecting $\hat{s}$ given that s is transmitted can be easily obtained by considering all possible signal points in the constellation, with the integration of the conditional p.d.f. of the received signal over the decision intervals mentioned above. The conditional PEP is given in general form as

$$\begin{aligned}P^e_{R_1}(a_i\to a_j)\Big|_{h_1}&=\int_{h_1\lambda_{j-1}}^{h_1\lambda_j} f_{y_{R_1}}(y_{R_1}\mid a_i,h_1)\,dy_{R_1}\\&=Q\left(\frac{h_1(\lambda_{j-1}-a_i)}{\psi}\right)-Q\left(\frac{h_1(\lambda_j-a_i)}{\psi}\right)\end{aligned} \tag{22}$$

for $i=1,\ldots,M$, $j\neq i$, $j\neq 1,M$. On the other hand, for the symbols at the rightmost and the leftmost of the constellation, we have

$$\begin{aligned}P^e_{R_1}(a_i\to a_1)\Big|_{h_1}&=\int_{-\infty}^{h_1\lambda_1} f_{y_{R_1}}(y_{R_1}\mid a_i,h_1)\,dy_{R_1}\\&=Q\left(\frac{h_1(a_i-\lambda_1)}{\psi}\right),\quad i\neq 1\end{aligned} \tag{23}$$

and,

$$\begin{aligned}P^e_{R_1}(a_i\to a_M)\Big|_{h_1}&=\int_{h_1\lambda_{M-1}}^{\infty} f_{y_{R_1}}(y_{R_1}\mid a_i,h_1)\,dy_{R_1}\\&=Q\left(\frac{h_1(\lambda_{M-1}-a_i)}{\psi}\right),\quad i\neq M.\end{aligned} \tag{24}$$

Using (19), $M_{h_1}(s)$ and (21), the unconditional PEP (UPEP) is derived as follows:

$$P^e_{R_1}(a_i\to a_j)=\begin{cases}q\left(\frac{(a_i-\lambda_1)^2}{N_0}\right), & j=1\\ \left|q\left(\frac{(\lambda_{j-1}-a_i)^2}{N_0}\right)-q\left(\frac{(\lambda_j-a_i)^2}{N_0}\right)\right|, & \text{o.w.}\\ q\left(\frac{(\lambda_{M-1}-a_i)^2}{N_0}\right), & j=M.\end{cases} \tag{25}$$

for $i=1,\ldots,M$, $j\neq i$.

Since coordinate interleaving technique with rotated M-QAM constellations allows us to distinguish symbols from only their real (or imaginary) parts, $P^c_{R_1}(s_1)=P^c_{R_1}\left(s_1^R\right)$ and $P^e_{R_1}(s_1\to\hat{s}_1)=P^e_{R_1}\left(s_1^R\to\hat{s}_1^R\right)$, for $s_1\neq\hat{s}_1$.

APPENDIX B
CALCULATION OF PROBABILITIES RELATED TO R_2 ($N=2$)
$P^c_{R_2}(s\mid R_1^c), P^e_{R_2}(s\to\hat{s}\mid R_1^c), P^e_{R_2}(s\to\hat{s}\mid R_1^e)$

i) $P^e_{R_2}(s_1\to\hat{s}_1\mid R_1^e)$: Considering that $s_1=s_1^R+js_1^I$ has been erroneously detected at R_1 as $\tilde{s}_1=\tilde{s}_1^R+j\tilde{s}_1^I$, the received signals at R_2 at the first two time slots is given as

$$\begin{bmatrix}r_{R_2}(1)\\ r_{R_2}(2)\end{bmatrix}=\begin{bmatrix}s_1^R+js_2^I & 0\\ 0 & s_2^R+j\tilde{s}_1^I\end{bmatrix}\begin{bmatrix}h_{SR_2}\\ h_{R_1R_2}\end{bmatrix}+\begin{bmatrix}n_{R_2}(1)\\ n_{R_2}(2)\end{bmatrix}. \tag{26}$$

As seen from (26), assuming correct detection at R_1, R_2 can be considered as the receiver of a 2×1 MISO system employing CIOD. Therefore, R_2 applies CIOD detection procedures to decode s_1 and s_2 by combining the received signals as: $\gamma_{R_2}=\alpha^R_{R_2}+j\beta^I_{R_2}$ and $\delta_{R_2}=\beta^R_{R_2}+j\alpha^I_{R_2}$, where $\alpha_{R_2}=h^*_{SR_2}r_{R_2}(1)$ and $\beta_{R_2}=h^*_{R_1R_2}r_{R_2}(2)$. Then, the ML decision rules for s_1 and s_2 are given as follows [10]: $\hat{s}_i=\arg\min_{s_i}\{m_{R_2}(s_i)\}$ for $i=1,2$, where

$$\begin{aligned}m_{R_2}(s_1)&=h_{1,2}\left(\gamma^R_{R_2}-h_2s_1^R\right)^2+h_2\left(\gamma^I_{R_2}-h_{1,2}s_1^I\right)^2,\\ m_{R_2}(s_2)&=h_2\left(\delta^R_{R_2}-h_{1,2}s_2^R\right)^2+h_{1,2}\left(\delta^I_{R_2}-h_2s_2^I\right)^2.\end{aligned}$$

The CPEP of detecting $\hat{s}_1$ when s_1 is transmitted can be written as

$$P^e_{R_2}(s_1\to\hat{s}_1\mid R_1^e)\Big|_{h_2,h_{1,2}}=P\left(m_{R_2}(\hat{s}_1)<m_{R_2}(s_1)\right). \tag{27}$$

Considering $\gamma_{R_2}=h_2s_1^R+jh_{1,2}\tilde{s}_1^I+w^R_{R_2}(1)+jw^I_{R_2}(2)$, where $w_{R_2}(1)=h^*_{SR_2}n_{R_2}(1)$ and $w_{R_2}(2)=h^*_{R_1R_2}n_{R_2}(2)$, we obtain

$$\begin{aligned}&P^e_{R_2}(s_1\to\hat{s}_1\mid R_1^e)\Big|_{h_2,h_{1,2}}=\\&P\Big(h_{1,2}\left[h_2\Delta_1+w^R_{R_2}(1)\right]^2+h_2\left[h_{1,2}\Delta_2+w^I_{R_2}(2)\right]^2\\&<h_{1,2}\left(w^R_{R_2}(1)\right)^2+h_2\left[h_{1,2}\Delta_3+w^I_{R_2}(2)\right]^2\Big)\end{aligned} \tag{28}$$

where $\Delta_1\triangleq s_1^R-\hat{s}_1^R$, $\Delta_2\triangleq\tilde{s}_1^I-\hat{s}_1^I$ and $\Delta_3\triangleq\tilde{s}_1^I-s_1^I$. After manipulation, we arrive at

$$P^e_{R_2}(s_1\to\hat{s}_1\mid R_1^e)\Big|_{h_2,h_{1,2}}=P(A<0) \tag{29}$$

where $A=h_2^2h_{1,2}\Delta_1^2+h_2h_{1,2}^2\left(\Delta_2^2-\Delta_3^2\right)+2h_2h_{1,2}\left[\Delta_1w^R_{R_2}(1)+(\Delta_2-\Delta_3)w^I_{R_2}(2)\right]$, and $A\sim\mathcal{N}\left(\mu_A,\sigma_A^2\right)$ with $\mu_A=h_2h_{1,2}\left(h_2\Delta_1^2+h_{1,2}\left(\Delta_2^2-\Delta_3^2\right)\right)$

and $\sigma_A^2 = 4\sigma^2 h_2^2 h_{1,2}^2 \left(h_2\Delta_1^2 + h_{1,2}\left(\Delta_2 - \Delta_3\right)^2\right)$. From (29), the desired CPEP expression can be obtained as

$$P_{R_2}^e(s_1 \to \hat{s}_1 \mid R_1^e)\Big|_{h_2,h_{1,2}} = Q\left(\frac{h_2\Delta_1^2 + h_{1,2}\left(\Delta_2^2 - \Delta_3^2\right)}{2\sigma\sqrt{h_2\Delta_1^2 + h_{1,2}\left(\Delta_2 - \Delta_3\right)^2}}\right). \tag{30}$$

Let us define $\Phi_1 = s_1^R - \hat{s}_1^R$ and $\Phi_2 = s_1^I - \hat{s}_1^I$. As we mentioned earlier, the average SEP at the destination is dominated by the case where $\tilde{s}_1 = \hat{s}_1$. Therefore, we have $\Delta_1^2 = \Phi_1^2$, $\Delta_2 = 0$ and $\Delta_3 = \Phi_2^2$ in (30), which gives

$$P_{R_2}^e\left(s_1 \to \hat{s}_1 \mid R_1^e\right)\Big|_{h_2,h_{1,2}} = Q\left(\frac{h_2\Phi_1^2 - h_{1,2}\Phi_2^2}{2\sigma\sqrt{h_2\Phi_1^2 + h_{1,2}\Phi_2^2}}\right). \tag{31}$$

We observe that (31) can take very large values when $h_{1,2}\Phi_2^2 > h_2\Phi_1^2$, which supports our assumption on $P_{R_2}^c\left(s \mid R_1^e\right) \ll P_{R_2}^e\left(s \to \hat{s} \mid R_1^e\right)$. Thus, we can approximate the UPEP for high SNR $(\sigma \to 0)$ as

$$P_{R_2}^e\left(s_1 \to \hat{s}_1 \mid R_1^e\right) \approx P\left(h_2\Phi_1^2 < h_{1,2}\Phi_2^2\right) \tag{32}$$

since the Q-function gives either unity or zero depending on the sign of the numerator for smaller values of σ. Let us define $u = u_1 - u_2$ where $u_1 \triangleq h_2\Phi_1^2$ and $u_2 \triangleq h_{1,2}\Phi_2^2$, then we obtain

$$P_{R_2}^e\left(s_1 \to \hat{s}_1 \mid R_1^e\right) \approx P\left(u < 0\right). \tag{33}$$

Considering the p.d.f.'s of u_1 and u_2 given as $f_{u_1}(u_1) = \left(2/\Phi_1^2\right)e^{-2u_1/\Phi_1^2}$ and $f_{u_2}(u_2) = \left(1/\Phi_2^2\right)e^{-u_2/\Phi_2^2}$ for $u_1 > 0$ and $u_2 > 0$, respectively, the p.d.f. of u, which is the difference of two exponential r.v.'s, can be calculated for $u < 0$ by [17]

$$\begin{aligned} f_u(u) &= \int_{-u}^{\infty} f_{u_1}(u+u_2)\, f_{u_2}(u_2)\, du_2 \\ &= \frac{2\exp\left(u/\Phi_2^2\right)}{\Phi_1^2 + 2\Phi_2^2} \end{aligned} \tag{34}$$

which yields

$$P_{R_2}^e\left(s_1 \to \hat{s}_1 \mid R_1^e\right) = \int_{-\infty}^{0} f_u(u)\, du = \frac{2\Phi_2^2}{\Phi_1^2 + 2\Phi_2^2}. \tag{35}$$

Eq. (35) proves that the probability of error becomes very high at R_2 if R_1 forwards an erroneously detected signal.

ii) $P_{R_2}^e\left(s_1 \to \hat{s}_1 \mid R_1^c\right)$: Assuming correct detection at R_1, the CPEP of detecting $\hat{s}_1$ when s_1 is transmitted can be obtained by setting $\tilde{s}_1^I = s_1^I$ in (30) $\left(\Delta_2^2 = \Phi_2^2, \Delta_3 = 0\right)$ as

$$P_{R_2}^e\left(s_1 \to \hat{s}_1 \mid R_1^c\right)\Big|_{h_2,h_{1,2}} = Q\left(\sqrt{\frac{h_2\Phi_1^2 + h_{1,2}\Phi_2^2}{2N_0}}\right) \tag{36}$$

which is the CPEP of the classical CIOD. Let us define $v = u_1 + u_2$ for $u_1 = h_2\Phi_1^2$ and $u_2 = h_{1,2}\Phi_2^2$. Using (19) and defining $M_v(s) = E\left\{e^{sv}\right\}$, the corresponding UPEP can be evaluated as follows:

$$P_{R_2}^e\left(s_1 \to \hat{s}_1 \mid R_1^c\right) = \frac{1}{\pi}\int_0^{\pi/2} M_v\left(\frac{-1}{4N_0\sin^2\theta}\right) d\theta. \tag{37}$$

Considering $f_{u_1}(u_1)$ and $f_{u_2}(u_2)$ given below of (33), the p.d.f. of v, which is the sum of two exponential r.v.'s, can be calculated by $(v > 0)$

$$\begin{aligned} f_v(v) &= \int_0^v f_{u_2}(u_2)\, f_{u_1}(v-u_2)\, du_2 \\ &= \frac{2\left(\exp\left(-2v/\Phi_1^2\right) - \exp\left(-v/\Phi_2^2\right)\right)}{\Phi_1^2 - 2\Phi_2^2}. \end{aligned} \tag{38}$$

Then, the corresponding m.g.f. is evaluated as

$$M_v(s) = \frac{2}{\left(\Phi_1^2 s - 2\right)\left(\Phi_2^2 s - 1\right)}. \tag{39}$$

Combining (37) and (39), and using Mathematica, we obtain

$$P_{R_2}^e\left(s_1 \to \hat{s}_1 \mid R_1^c\right) = \frac{\Phi_1^2\left(1-\rho_1\right) + 2\Phi_2^2\left(-1+\rho_2\right)}{2\left(\Phi_1^2 - 2\Phi_2^2\right)} \tag{40}$$

where $\rho_1 \triangleq 1/\sqrt{1 + 8N_0/\Phi_1^2}$ and $\rho_2 \triangleq 1/\sqrt{1 + 4N_0/\Phi_2^2}$. Note that (40) differs from the UPEP of the classical CIOD operating on uncorrelated Rayleigh fading channels due to the different p.d.f. of h_2.

iii) $P_{R_2}^c\left(s_1 \mid R_1^c\right)$: The correct detection probability of s_1 at R_2 given that R_1 forwarded the correct s_1 component, can be easily obtained by using (40) in the following union bound:

$$P_{R_2}^c\left(s_1 \mid R_1^c\right) \le 1 - \frac{1}{M}\sum_{\hat{s}_1, \hat{s}_1 \neq s_1} P_{R_2}^e\left(s_1 \to \hat{s}_1 \mid R_1^c\right). \tag{41}$$

APPENDIX C
CALCULATION OF PROBABILITIES RELATED WITH D $(N = 2)$

$$P_D\left(s \to \hat{s} \mid R_1^c, R_2^c\right), P_D\left(s \to \hat{s} \mid R_1^c, R_2^e\right), P_D\left(s \to \hat{s} \mid R_1^e, R_2^e\right)$$

i) $P_D\left(s_1 \to \hat{s}_1 \mid R_1^e, R_2^e\right)$: Assuming that $s_1 = s_1^R + js_1^I$ has been erroneously detected as $\tilde{s}_1 = \tilde{s}_1^R + j\tilde{s}_1^I$ and $\bar{s}_1 = \bar{s}_1^R + j\bar{s}_1^I$ at R_1 and R_2, respectively, the received signals at the destination for $t = 2$ and 3 can be expressed as

$$\begin{bmatrix} r_D(3) \\ r_D(2) \end{bmatrix} = \begin{bmatrix} \bar{s}_1^R + js_2^I & 0 \\ 0 & s_2^R + j\tilde{s}_1^I \end{bmatrix}\begin{bmatrix} h_{R_2D} \\ h_{R_1D} \end{bmatrix} + \begin{bmatrix} n_D(3) \\ n_D(2) \end{bmatrix}. \tag{42}$$

According to the CIOD detection procedures, after processing and interleaving these signals as $\alpha_D = h_{R_2D}^* r_D(3)$, $\beta_D = h_{R_1D}^* r_D(2)$ and, $\gamma_D = \alpha_D^R + j\beta_D^I$, $\delta_D = \beta_D^R + j\alpha_D^I$, respectively, the receiver calculates the ML decision metrics as

$$\begin{aligned} \hat{s}_1 &= \arg\min_{s_1}\left\{g_1\left(\gamma_D^R - g_2 s_1^R\right)^2 + g_2\left(\gamma_D^I - g_1 s_1^I\right)^2\right\}, \\ \hat{s}_2 &= \arg\min_{s_2}\left\{g_2\left(\delta_D^R - g_1 s_2^R\right)^2 + g_1\left(\delta_D^I - g_2 s_2^I\right)^2\right\}. \end{aligned} \tag{43}$$

Considering $\gamma_D = g_2\bar{s}_1^R + jg_1\tilde{s}_1^I + w_D^R(3) + jw_D^I(2)$ where $w_D(3) = h_{R_2D}^* n_D(3)$ and $w_D(2) = h_{R_1D}^* n_D(2)$, similarly to (27), the CPEP can be calculated as

$$\begin{aligned} &P_D\left(s_1 \to \hat{s}_1 \mid R_1^e, R_2^e\right)\Big|_{g_1,g_2} = \\ &\quad P\Big(g_1\left[g_2\Delta_4 + w_D^R(3)\right]^2 + g_2\left[g_1\Delta_2 + w_D^I(2)\right]^2 \\ &\quad < g_1\left[g_2\Delta_5 + w_D^R(3)\right]^2 + g_2\left[g_1\Delta_3 + w_D^I(2)\right]^2\Big) \end{aligned} \tag{44}$$

where Δ_2 and Δ_3 are defined in (28), and $\Delta_4 \triangleq \bar{s}_1^R - \hat{s}_1^R$, $\Delta_5 \triangleq \bar{s}_1^R - s_1^R$. After simple calculations, we obtain

$$P_D\left(s_1 \to \hat{s}_1 \mid R_1^e, R_2^e\right)\Big|_{g_1,g_2} = P\left(B < 0\right) \tag{45}$$

where $B = g_1 g_2^2 \left(\Delta_4^2 - \Delta_5^2\right) + g_1^2 g_2 \left(\Delta_2^2 - \Delta_3^2\right) + 2 g_1 g_2 \left[\left(\Delta_4 - \Delta_5\right) w_D^R(3) + \left(\Delta_2 - \Delta_3\right) w_D^I(2)\right]$ and $B \sim \mathcal{N}\left(\mu_B, \sigma_B^2\right)$ with $\mu_B = g_1 g_2 \Big(g_2 \left(\Delta_4^2 - \Delta_5^2\right) + g_1 \left(\Delta_2^2 - \Delta_3^2\right) \Big)$ and $\sigma_B^2 = 4\sigma^2 g_1^2 g_2^2 \Big(g_2 \left(\Delta_4 - \Delta_5\right)^2 + g_1 \left(\Delta_2 - \Delta_3\right)^2 \Big)$. Then, the corresponding UPEP can be expressed as

$$P_D\left(s_1 \to \hat{s}_1 \mid R_1^e, R_2^e\right)\Big|_{g_1,g_2} = Q\left(\frac{g_2\left(\Delta_4^2 - \Delta_5^2\right) + g_1\left(\Delta_2^2 - \Delta_3^2\right)}{2\sigma\sqrt{g_2\left(\Delta_4 - \Delta_5\right)^2 + g_1\left(\Delta_2 - \Delta_3\right)^2}}\right). \quad (46)$$

As mentioned earlier, we assume that for the dominant case $\bar{s}_1^R = \hat{s}_1^R$, $\tilde{s}_1^I = \hat{s}_1^I$, which gives $\Delta_2 = \Delta_4 = 0$, $\Delta_5^2 = \Phi_1^2$ and $\Delta_3^2 = \Phi_2^2$, for which (46) simplifies to

$$P_D\left(s_1 \to \hat{s}_1 \mid R_1^e, R_2^e\right)\Big|_{g_1,g_2} = Q\left(-\sqrt{\frac{g_2\Phi_1^2 + g_1\Phi_2^2}{2N_0}}\right) = 1 - P_D\left(s_1 \to \hat{s}_1 \mid R_1^c, R_2^c\right)\Big|_{g_1,g_2} \quad (47)$$

where $P_D\left(s_1 \to \hat{s}_1 \mid R_1^c, R_2^c\right)\big|_{g_1,g_2}$ is equal to the CPEP of the classical CIOD, which will be calculated in the sequel. As seen from (47), the error probability approaches unity with increasing SNR, which is expected since both relays erroneously detected s_1 and forwarded this signal to D.

ii) $P_D\left(s_1 \to \hat{s}_1 \mid R_1^c, R_2^e\right)$: Assuming that $s_1 = s_1^R + j s_1^I$ has been correctly detected at R_1 ($\tilde{s}_1 = s_1$) and erroneously detected as $\hat{s}_1 = \hat{s}_1^R + j\hat{s}_1^I$ at R_2 ($\bar{s}_1 = \hat{s}_1$), by setting $\Delta_3 = \Delta_4 = 0, \Delta_2^2 = \Phi_2^2$ and $\Delta_5^2 = \Phi_1^2$ in (46), we obtain

$$P_D\left(s_1 \to \hat{s}_1 \mid R_1^c, R_2^e\right)\Big|_{g_1,g_2} = Q\left(\frac{-g_2\Phi_1^2 + g_1\Phi_2^2}{2\sigma\sqrt{g_2\Phi_1^2 + g_1\Phi_2^2}}\right) \quad (48)$$

which has a similar structure as that of (31), and the corresponding UPEP can be calculated as

$$P_D\left(s_1 \to \hat{s}_1 \mid R_1^c, R_2^e\right) \approx P\left(g_1\Phi_2^2 < g_2\Phi_1^2\right) = \frac{\Phi_1^2}{\Phi_1^2 + \Phi_2^2}. \quad (49)$$

iii) $P_D\left(s_1 \to \hat{s}_1 \mid R_1^c, R_2^c\right)$: Assuming that both of the relays have successfully detected s_1, i.e., $\tilde{s}_1 = s_1$ and $\bar{s}_1 = s_1$, we have $\Delta_3 = \Delta_5 = 0$, $\Delta_4^2 = \Phi_1^2$ and $\Delta_2^2 = \Phi_2^2$, and (46) simplifies to the CPEP of the classical CIOD as

$$P_D\left(s_1 \to \hat{s}_1 \mid R_1^c, R_2^c\right)\Big|_{g_1,g_2} = Q\left(\sqrt{\frac{g_2\Phi_1^2 + g_1\Phi_2^2}{2N_0}}\right) \quad (50)$$

for which the UPEP can be calculated as follows:

$$P_D\left(s_1 \to \hat{s}_1 \mid R_1^c, R_2^c\right) = \frac{1}{\pi}\int_0^{\pi/2} M_w\left(\frac{-1}{4N_0\sin^2\theta}\right) d\theta \quad (51)$$

where $w \triangleq g_2\Phi_1^2 + g_1\Phi_2^2$ with p.d.f. and m.g.f. given respectively as

$$f_w(w) = \frac{\exp\left(-w/\Phi_1^2\right) - \exp\left(-w/\Phi_2^2\right)}{\Phi_1^2 - \Phi_2^2}, w > 0$$
$$M_w(s) = \frac{1}{\left(\Phi_1^2 s - 1\right)\left(\Phi_2^2 s - 1\right)}. \quad (52)$$

Substituting (52) in (51), the desired UPEP value can be calculated as

$$P_D\left(s_1 \to \hat{s}_1 \mid R_1^c, R_2^c\right) = \frac{\Phi_1^2\left(1 - \rho_1\right) + \Phi_2^2\left(-1 + \rho_2\right)}{2\left(\Phi_1^2 - \Phi_2^2\right)} \quad (53)$$

where $\rho_1 \triangleq 1/\sqrt{1 + 4N_0/\Phi_1^2}$ and $\rho_2 \triangleq 1/\sqrt{1 + 4N_0/\Phi_2^2}$. Note that (53) is the UPEP of the classical CIOD operating on uncorrelated Rayleigh fading channels.

APPENDIX D
DIVERSITY GAIN ANALYSIS FOR $N = 2$

In this appendix, we derive the diversity gain of the proposed protocol from (6) for $N = 2$, while using very similar procedures, generalizations to other networks are possible. Using the relationship between the ASEP and SNR (or noise power N_0 for a fixed signal power), the diversity gain of the system can be calculated using [18]

$$G_d = -\lim_{N_0 \to 0} \frac{\log\left(P_D\left(s \to \hat{s}\right)\right)}{\log\left(1/N_0\right)}. \quad (54)$$

Since $P_D\left(s \to \hat{s}\right)$ given in (6) contains many conditional terms, the application of (54) to $P_D\left(s \to \hat{s}\right)$ for high SNR ($N_0 \to 0$) is not straightforward. For high SNR, the correct detection probabilities $P_{R_1}^c(s)$ and $P_{R_2}^c\left(s \mid R_1^c\right)$ in (6) approach unity and can be discarded. It is observed from (47) that $P_D\left(s_1 \to \hat{s}_1 \mid R_1^e, R_2^e\right)$ also approaches unity with increasing SNR, and as seen from (35) and (49) respectively, $P_{R_2}^e\left(s_1 \to \hat{s}_1 \mid R_1^e\right)$ and $P_D\left(s_1 \to \hat{s}_1 \mid R_1^c, R_2^e\right)$ are constant terms which do not depend on the SNR and cannot effect the diversity order. Therefore, (6) can be simplified as

$$P_D\left(s \to \hat{s}\right) \propto P_D\left(s \to \hat{s} \mid R_1^c, R_2^c\right) + P_{R_2}^e\left(s \to \hat{s} \mid R_1^c\right) + P_{R_1}^e\left(s \to \hat{s}\right) \quad (55)$$

for diversity order calculation. Please note that the three terms in (55) are given in (53), (36) and (25), respectively. Applying (54) to each term of (55) and using numerical methods, for which details are omitted here due to space restrictions, it can be shown that $G_d = 2$ is obtained for each of these terms. This proves that our scheme achieves a diversity order of two which is also validated by the slopes of the theoretical curves given in Fig. 4.

APPENDIX E
CALCULATION OF ASEP FOR $N = 3$

For the three-relay case, considering the p.d.f.'s of $h_i, i = 1, 2, 3$ given as $f_{h_1}(h_1) = 3\left(1 - e^{-h_1}\right)^2 e^{-h_1}$, $f_{h_2}(h_2) = 6\left(1 - e^{-h_2}\right) e^{-2h_2}$, and $f_{h_3}(h_3) = 3e^{-3h_3}$ for $h_i > 0$, obtained from (13), the corresponding probabilities in (7) can be obtained with slight modifications of the results obtained in Appendices A, B and C as follows. Please note that the probabilities related to D are the same as those for the two-relay network (Appendix C) since the corresponding channel statistics (between the relay nodes and D) are identical for both schemes regardless of the number of relays in the network.

i) $P_{R_1}^c(s_1)$ and $P_{R_1}^e\left(s_1 \to \hat{s}_1\right)$: These two probabilities can be calculated from (20) and (25), respectively; however, for

this case, due to the different statistics of h_1, we use the new $q(x)$ function defined as

$$q(x) \triangleq \frac{1}{\pi}\int_0^{\pi/2} M_{h_1}\left(\frac{-x}{\sin^2\theta}\right)d\theta = \frac{1}{2}\left(1-\frac{3}{\sqrt{1+\frac{1}{x}}}+\frac{3}{\sqrt{1+\frac{2}{x}}}-\frac{1}{\sqrt{1+\frac{3}{x}}}\right) \quad (56)$$

where

$$M_{h_1}(s) = \frac{6}{6-11s+6s^2-s^3}. \quad (57)$$

ii) $P^e_{R_2}(s_1 \to \hat{s}_1 \mid R_1^e)$: This probability can be calculated by following the same steps as those in Appendix B as

$$P^e_{R_2}(s_1 \to \hat{s}_1 \mid R_1^e) = \int_{-\infty}^{0} f_u(u)\,du = \frac{6\Phi_2^4}{\Phi_1^4+5\Phi_1^2\Phi_2^2+6\Phi_2^4} \quad (58)$$

where u is as defined in (33) and due to the different p.d.f. of h_2, instead of (34), we have used

$$f_u(u) = \frac{6\exp\left(u/\Phi_2^2\right)\Phi_2^2}{\Phi_1^4+5\Phi_1^2\Phi_2^2+6\Phi_2^4}, \quad u<0, \quad (59)$$

for the three-relay case.

iii) $P^e_{R_2}(s_1 \to \hat{s}_1 \mid R_1^c)$: This probability can be calculated from (37) by using

$$M_v(s) = \frac{-6}{(\Phi_1^2 s-3)(\Phi_1^2 s-2)(\Phi_2^2 s-1)} \quad (60)$$

where v is as defined in (37). Due to space limitations, the result obtained by combining (37) and (60) is omitted here. Interested readers can obtain the desired closed form result by using Mathematica software. ■

As seen from Table II, the transmission of the symbols s_3 and s_4 is very similar to that of s_1 and s_2, where only the secondary (supporting) relays are different. In other words, the symbol pair (s_1, s_2) is transferred to D via R_1 and R_2, while the symbol pair (s_3, s_4) is transferred to D via R_1 and R_3. On the other hand, for simplicity, we do not consider the effects of the possible interference caused by the erroneous detection of s_1 and s_2 at the relay nodes, on the error performance of s_3 and s_4 in our analytical calculations.

iv) $P^c_{R_3}(s_3)$ and $P^e_{R_3}(s_3 \to \hat{s}_3)$: These probabilities are the same as those for s_1 given above and can be calculated by (20) and (25), respectively, using (56).

v) $P^e_{R_3}(s_3 \to \hat{s}_3 \mid R_1^e)$: This probability can be calculated by following the same steps as those in Appendix B as

$$P^e_{R_3}(s_3 \to \hat{s}_3 \mid R_1^e) = \int_{-\infty}^{0} f_u(u)\,du = \frac{3\Phi_2^2}{\Phi_1^2+3\Phi_2^2}. \quad (61)$$

where for this case, $u \triangleq h_3\Phi_1^2 - h_{13}\Phi_2^2$ with p.d.f.

$$f_u(u) = \frac{3\exp\left(u/\Phi_2^2\right)}{\Phi_1^2+3\Phi_2^2}, \quad u<0. \quad (62)$$

vi) $P^e_{R_3}(s_3 \to \hat{s}_3 \mid R_1^c)$: This probability can be calculated by using (37), where for three relays, $v \triangleq h_3\Phi_1^2 + h_{13}\Phi_2^2$ with the corresponding m.g.f.

$$M_v(s) = \frac{3}{(\Phi_1^2 s-3)(\Phi_2^2 s-1)}. \quad (63)$$

By combining (37) and (63), we obtain

$$P^e_{R_3}(s_3 \to \hat{s}_3 \mid R_1^c) = \frac{\Phi_1^2(1-\rho_1)+3\Phi_2^2(-1+\rho_2)}{2(\Phi_1^2-3\Phi_2^2)} \quad (64)$$

where $\rho_1 \triangleq 1/\sqrt{1+12N_0/\Phi_1^2}$ and $\rho_2 \triangleq 1/\sqrt{1+4N_0/\Phi_2^2}$.

APPENDIX F
CALCULATION OF THE APPROXIMATE ASEP FOR GENERAL N

Although it seems quite complicated to obtain exact closed form ASEP expressions for general N values, we use induction to obtain the results given in this appendix.

Similar to the previous cases, probabilities related with R_1 are identical for s_1 and s_{2N-3}, and the corresponding probabilities $P^c_{R_1}(s_i)$ and $P^e_{R_1}(s_i \to \hat{s}_i)$ for $i=1$ and $2N-3$ can be calculated from (20) and (25), respectively, where for N relays we have

$$q(x) \triangleq \frac{1}{2}\sum_{j=0}^{N}\frac{(-1)^j\binom{N}{j}}{\sqrt{1+\frac{j}{x}}}. \quad (65)$$

A. New Calculations for $P_D(s_1 \to \hat{s}_1)$

By generalizing our previous calculations, we obtain

$$P^e_{R_2}(s_1 \to \hat{s}_1 \mid R_1^e) = \frac{N!\Phi_2^{2(N-1)}}{\prod_{i=2}^{N}(\Phi_1^2+i\Phi_2^2)} \quad (66)$$

while $P^e_{R_2}(s_1 \to \hat{s}_1 \mid R_1^c)$ can be calculated using (37), where

$$M_v(s) = \frac{(-1)^N N!}{(\Phi_2^2 s-1)\prod_{i=2}^{N}(\Phi_1^2 s-i)}. \quad (67)$$

Unfortunately, a closed from solution cannot be found for the combination of (37) and (67) for general N values, and numerical integration has to be considered.

B. New Calculations for $P_D(s_{2N-3} \to \hat{s}_{2N-3})$

For N relays, by generalizing our previous derivations, we obtain

$$P^e_{R_N}(s_{2N-3} \to \hat{s}_{2N-3} \mid R_1^e) = \frac{N\Phi_2^2}{\Phi_1^2+N\Phi_2^2}, \quad (68)$$

$$P^e_{R_N}(s_{2N-3} \to \hat{s}_{2N-3} \mid R_1^c) = \frac{\Phi_1^2(1-\rho_1)+N\Phi_2^2(-1+\rho_2)}{2(\Phi_1^2-N\Phi_2^2)} \quad (69)$$

where $\rho_1 \triangleq 1/\sqrt{1+4NN_0/\Phi_1^2}$ and $\rho_2 \triangleq 1/\sqrt{1+4N_0/\Phi_2^2}$.

REFERENCES

[1] J. Laneman and G. Wornell, "Distributed space-time-coded protocols for exploiting cooperative diversity in wireless networks," *IEEE Trans. Inf. Theory*, vol. 49, no. 10, pp. 2415–2425, Oct. 2003.

[2] J. Laneman, D. Tse, and G. W. Wornell, "Cooperative diversity in wireless networks: efficient protocols and outage behavior," *IEEE Trans. Inf. Theory*, vol. 50, no. 12, pp. 3062–3080, Dec. 2004.

[3] A. Sendonaris, E. Erkip, and B. Aazhang, "User cooperation diversity—part I: system description," *IEEE Trans. Commun.*, Nov. 2003.

[4] Y. Jing and B. Hassibi, "Distributed space-time coding in wireless relay networks," *IEEE Trans. Wireless Commun.*, vol. 5, no. 12, pp. 3524–3536, Dec. 2006.

[5] Z. Ding, I. Krikidis, B. Rong, J. Thompson, C. Wang, and S. Yang, "On combating the half-duplex constraint in modern cooperative networks: protocols and techniques," *IEEE Wireless Commun. Mag.*, vol. 19, no. 6, pp. 20–27, Dec. 2012.
[6] B. Rankov and A. Wittneben, "Spectral efficient protocols for half-duplex fading relay channels," *IEEE J. Sel. Areas Commun.*, vol. 25, no. 2, pp. 379–389, Feb. 2007.
[7] Y. Fan, C. Wang, J. Thompson, and H. V. Poor, "Recovering multiplexing loss through successive relaying using repetition coding," *IEEE Trans. Wireless Commun.*, vol. 6, no. 12, pp. 4484–4493, Dec. 2007.
[8] F. Tian, W. Zhang, W.-K. Ma, P. Ching, and H. V. Poor, "An effective distributed space-time code for two-path successive relay network," *IEEE Trans. Commun.*, vol. 59, no. 8, pp. 2254–2263, Aug. 2011.
[9] L. Shi, W. Zhang, and P. C. Ching, "Single-symbol decodable distributed STBC for two-path successive relay networks," in *Proc. 2011 IEEE Int. Conf. on Acoustics, Speech and Signal Proc.*, pp. 3324–3327.
[10] M. Z. A. Khan and B. S. Rajan, "Single-symbol maximum likelihood decodable linear STBCs," *IEEE Trans. Inf. Theory*, vol. 52, no. 5, pp. 2062–2091, May 2006.
[11] N. Sadeque, I. Land, and R. Subramanian, "A successive relaying protocol for a cooperative three-relay network," in *Proc. 2012 Australian Communications Theory Workshop*, pp. 72–77.
[12] C. Luo, Y. Gong, and F. Zheng, "Full interference cancellation for two-path cooperative communications," in *Proc. 2009 IEEE Wireless Commun. and Networking Conf.*, pp. 1–5.
[13] W. Chen, Z. Chen, and C. Zhou, "Joint source-relay optimization for two-path MIMO AF relay system," in *Proc. 2012 Int. Conf. on Wireless Commun., Networking and Mobile Computing*, pp. 1–5.
[14] H. Wicaksana, S. Ting, Y. Guan, and X. G. Xia, "Decode-and-forward two-path half-duplex relaying: diversity-multiplexing tradeoff analysis," *IEEE Trans. Commun.*, vol. 59, no. 7, pp. 1985–1994, Jul. 2011.
[15] J. Wu and C. Xiao, "Optimal diversity combining based on linear estimation of Rician fading channels," *IEEE Trans. Commun.*, vol. 56, no. 10, pp. 1612–1615, Oct. 2008.
[16] W. Gifford, M. Win, and M. Chiani, "Diversity with practical channel estimation," *IEEE Trans. Wireless Commun.*, vol. 4, no. 4, pp. 1935–1947, Jul. 2005.
[17] A. Papoulis and S. U. Pillai, *Probability, Random Variables and Stochastic Processes*, 4th ed. McGraw-Hill, Inc., 2002.
[18] H. Jafarkhani, *Space-Time Coding*. Cambridge University Press, 2005.

Ertuğrul Başar (S'09–M'13) was born in Istanbul, Turkey, in 1985. He received the B.S. degree from Istanbul University, Istanbul, Turkey, in 2007, and the M.S. and Ph.D. degrees from the Istanbul Technical University, Istanbul, Turkey, in 2009 and 2013, respectively. Dr. Başar spent the academic year 2011-2012 in the Department of Electrical Engineering, Princeton University, New Jersey, USA. Currently, he is a research assistant at Istanbul Technical University. His primary research interests include MIMO systems, space-time coding, spatial modulation systems, OFDM and cooperative diversity.

Ümit Aygölü (M'90) received his B.S., M.S. and Ph.D. degrees, all in electrical engineering, from Istanbul Technical University, Istanbul, Turkey, in 1978, 1984 and 1989, respectively. He was a Research Assistant from 1980 to 1986 and a Lecturer from 1986 to 1989 at Yildiz Technical University, Istanbul, Turkey. In 1989, he became an Assistant Professor at Istanbul Technical University, where he became an Associate Professor and Professor, in 1992 and 1999, respectively. His current research interests include the theory and applications of combined channel coding and modulation techniques, MIMO systems, space-time coding, cooperative communication and spatial modulation.

Erdal Panayırcı (M'80–SM'91–F'2003–LF'2006) received the Diploma Engineering degree in Electrical Engineering from Istanbul Technical University, Istanbul, Turkey and the Ph.D. degree in Electrical Engineering and System Science from Michigan State University, USA. Until 1998 he has been with the Faculty of Electrical and Electronics Engineering at the Istanbul Technical University, where he was a Professor and Head of the Telecommunications Chair. Currently, he is Professor of Electrical Engineering and Head of the Electronics Engineering Department at Kadir Has University, Istanbul, Turkey. Dr. Panayirci's recent research interests include communication theory, synchronization, advanced signal processing techniques and their applications to wireless communications. coded modulation and interference cancellation in heterogeneous networks . He has published extensively in leading scientific journals and international conference and co-authored the book Principles of Integrated Maritime Surveillance Systems (Boston, Kluwer Academic Publishers, 2000).

Dr. Panayırcı spent the academic year 2008-2009 at the Department of Electrical Engineering, Princeton University, New Jersey, USA, working on new channel estimation and equalization algorithms for high mobility WIMAX and LTE systems. He has been the principal coordinator of a 6th and 7th Frame European project called NEWCOM (Network of Excellent on Wireless Communications) representing Kadir Has University for five years and WIMAGIC Strep project for two years. Prof. Panayirci was an Editor for IEEE Transactions on Communications in the areas of Synchronizations and Equalizations in 1995-1999. He served as a Member of IEEE Fellow Committee in 2005-2008. He was the Technical Program Co-Chair of the IEEE International Conference on Communications (ICC-2006) and the Technical Program Chair of the IEEE PIMRC held in Istanbul, Turkey both held in Istanbul in 2006 and 2010, respectively. He is the Executive Vice Chairman of the upcoming IEEE Wireless Communications and Networking Conference (WCNC) to be held in Istanbul in April 2014. Presently he is head of the Turkish Scientific Commission on Signals and Systems of URSI (International Union of Radio Science).

H. Vincent Poor (S'72–M'77–SM'82–F'87) received the Ph.D. degree in EECS from Princeton University in 1977. From 1977 until 1990, he was on the faculty of the University of Illinois at Urbana-Champaign. Since 1990 he has been on the faculty at Princeton, where he is the Michael Henry Strater University Professor of Electrical Engineering and Dean of the School of Engineering and Applied Science. Dr. Poor's research interests are in the areas of information theory, statistical signal processing and stochastic analysis, and their applications in wireless networks and related fields including social networks and smart grid. Among his publications in these areas are the recent books *Principles of Cognitive Radio* (Cambridge University Press, 2013) and *Mechanisms and Games for Dynamic Spectrum Allocation* (Cambridge University Press, 2014).

Dr. Poor is a member of the National Academy of Engineering, the National Academy of Sciences, and Academia Europaea, and is a fellow of the American Academy of Arts and Sciences, the Royal Academy of Engineering (U. K), and the Royal Society of Edinburgh. He received the Marconi and Armstrong Awards of the IEEE Communications Society in 2007 and 2009, respectively. Recent recognition of his work includes the 2010 IET Ambrose Fleming Medal for Achievement in Communications, the 2011 IEEE Eric E. Sumner Award, and honorary doctorates from Aalborg University, the Hong Kong University of Science and Technology, and the University of Edinburgh.